Desalination and Water Treatment
www.deswater.com
doi: 10.5004/dwt.2019.24039

154 (2019) 347–355
June

Efficiency of the activated carbon and clinoptilolite particles coated with iron oxide magnetic nanoparticles in removal of methylene blue

Ahmad Badeenezhad[a,b], Abooalfazl Azhdarpoor[a,*]

[a]*School of Health, Shiraz University of Medical Sciences, Shiraz, Iran, emails: Azhdarpoor@sums.ac.ir (A. Azhdarpoor), ahmadbadee72@gmail.com (A. Badeenezhad)*
[b]*Department of Environmental Health Engineering, School of Health, Behbahan Faculty of Medical Sciences, Behbahan, Iran*

Received 29 August 2018; Accepted 27 February 2019

ABSTRACT

Due to the toxicity, carcinogenicity and low biodegradability of organic dyes, removing them from wastewaters is essential. In this respect, this study synthesized the iron oxide coated activated carbon and zeolite (clinoptilolite) adsorbents. Two adsorbents were applied to remove methylene blue and the corresponding parameters, including solution pH, adsorbent dose, initial dye concentration, and contact time, were optimized. According to the findings, the optimal contact time for the clinoptilolite and activated carbon magnetic nanoparticles was, respectively, 45 and 30 min. Meanwhile, pH did not significantly affect the adsorption process though changing pH from 7 to 9 which reduced the adsorption efficiency of the clinoptilolite magnetic nanoparticles from 98.6% to 96%. The prepared activated carbon and clinoptilolite adsorbents were so efficient that they remove 99% and 98.3% of the methylene blue from 100 ppm dye solutions, at pH 7. In general, the results demonstrated that coating the activated carbon and clinoptilolite particles with the Fe_2O_3 nanoparticles was effective in enhancing their efficiency of methylene blue removal from aqueous solutions within short times.

Keywords: Methylene blue; Adsorbent; Clinoptilolite; Activated carbon; Iron oxide

1. Introduction

Over the last decades, the environment has been extensively polluted by the dye-containing wastewaters that mainly originate from the textile, leather, dyeing, and paper industries [1]. However, most dyes are designed and produced as complicated synthetic structures to maintain their stability over long periods and/or withstand against oxidation by solar radiation and oxidant agents. That is why most dyes cannot be degraded through conventional wastewater treatment processes [2]. Among various dyes, methylene blue (MB) has been commonly used in many industrial applications [3], such as production of colored paper, and dyeing hair, cotton, and wool [4].

The wastewaters contaminated by MB and similar dyes are of utmost importance since their emission to the ecosystem can alter the appearance of water resources and interrupt the life of aquatic species [5]. In this respect, many methods have been suggested to remove MB from water and wastewater, including coagulation and flocculation [3], membrane-based separation, oxidation and ozonation, electrical coagulation, and adsorption [6–8]. Among these techniques, adsorption has been proven to be more efficient from the perspectives of design, utilization, high removal capacity, insensitivity to toxic compounds, facile recovery, and low price [8–10].

However, the key to a successful adsorption process is the application of an appropriate adsorbent. The potential adsorbents, activated carbon (AC) and clinoptilolite, have been recently studied by many researchers. Though AC has many fine pores to help remove pollutants, its efficiency can be further improved [11]. Activated carbon, due to its

* Corresponding author.

structure and high surface area, has been proposed as an adsorbent in air and water pollution control and catalytic supports in the chemical and petrochemical industries, and it is a suitable option for the effective removal of organic contaminations (especially hard-biodegradable pollutants) from aquatic environment, because of their high specific surface area, porosity, chemical inertness, and thermal stability. However, its use in large scales (in engineering processes) has been limited because of such problems as filtration, dispersion, creation of turbidity, and high cost of its reduction [12–14]. Also, zeolites, which are highly porous inorganic compounds composed of aluminum silicate and proper adsorption properties, have been used as commercial adsorbents. To promote the adsorption efficiency of these adsorbents, many researchers have shifted toward adsorbent modification [15]. Though there are several approaches available to modify adsorbents, the formation of nanoparticles (NPs) has attracted more interest since it provides a high surface to volume ratio for the removal of organic compounds. However, separation of NPs from aqueous media is difficult. Therefore, separability of the adsorbent NPs should be improved by fixating them on different supports, for example, oxides, polymers, AC, and inorganic adsorbents. In this way, the use of adsorbent NPs would be more practical and economic [16]. Particularly, applicability, separability, and efficiency of the NPs would be enhanced if they present magnetic properties [17].

Though many recent studies have attempted to promote the efficiency of adsorbents in the removal of various pollutants, specifically MB, from aqueous solutions using different adsorbents including modified bamboo hydrochar, chitosan, titanium composites, calcium alginate, modified ash, and rice husk [3,18–21], more advances are expected. For instance, coating of appropriate adsorbents, such as AC and clinoptilolite, by magnetic nanoparticles (MNPs) is expected to generate ideal adsorbents with a higher capacity of dye adsorption.

Clinoptilolite is known as a natural adsorbent that is widely distributed and abundantly found in nature. Hence, it is available as an affordable adsorbent. Also, its preparation and modification cost as used in this study was relatively inexpensive. Therefore, this method can significantly increase the clinoptilolite capacity adsorption as a cheap adsorbent. In this method, it has been attempted to compare the adsorption capacity of clinoptilolite with activated carbon that is a commonly and widely used and an attractive adsorbent.

Since the AC and clinoptilolite adsorbents have a low tendency toward MB removal from wastewater, the objective of the present study was to promote their removal efficiency through coating the AC and clinoptilolite particles by iron oxide MNPs.

2. Materials and methods

2.1. Materials

Analytical grade MB ($C_{16}H_{18}N_3ClS$), $FeCl_3.6H_2O$, $FeSO_4.7H_2O$, NaOH and AC were purchased from Merck Co., (Germany). The clinoptilolite was supplied by a mine located in Semnan, Iran. The supplied zeolite was milled and passed through a standard ASTM filter to reach the particles with 400 μm.

2.2. Synthesis of the magnetic nanoparticle–coated activated carbon and clinoptilolite

To synthesize the MNPs [22], 5 g of each adsorbent (powdered AC and the zeolite), 6.1 g iron chloride ($FeCl_3.6H_2O$) and 4.2 g iron sulfate ($FeSO_4.7H_2O$) were added to 100 mL distilled water in a 250 mL beaker and ultrasonicated by a GOH2-ELMA ultrasonication device. After that, the pH level of the suspension was adjusted at 10 using 0.1 N NaOH, and the basic mixture was stirred for 24 h at 160 rpm and at room temperature. Then, 25 mL of a NaOH solution (6.5 M) was gently added to the resultant suspension and stirred for 1 h. The obtained solid particles were washed several times with distilled water and heated in an oven at 300°C to activate the modified NPs.

2.3. Adsorption experiments

An MB solution with 2,000 ppm concentration was prepared as the stock solution and diluted to make the other solutions with different concentrations. The adsorption experiments were performed in a batch system containing 50 mL sample with 50 ppm concentration and 0.5 g adsorbent per 50 mL of the solution. The system contents were stirred for 45 min at 120 rpm and at room temperature. The pH levels of the examined solutions were adjusted using 0.1 N HCl and/or NaOH and measured by a Metrohm (Switzerland) pH meter. The adsorption process was optimized with respect to the adsorbent dose (0.1, 0.3, 0.5, 0.7, and 1 g per 50 mL of the solution), initial MB concentration (25, 50, 75, 100, 150, and 200 ppm), pH (3, 5, 7, and 9), and the contact time (5, 15, 30, 45, 60, and 90 min) by varying just one parameter and fixing the others at each trial. Also, the kinetics and isotherms of the process were studied. To analyze the samples and measure the residual dyes, a DR5000 UV/Vis spectrophotometer (HACH Co., USA) was used and the absorption intensity of the samples was recorded at the maximum wavelength of MB, that is, 665 nm. All the experiments were repeated three times and the average results were reported. To prevent any error in the obtained results, all utilized equipments were washed with acid and later with distilled water.

The equilibrium adsorption data were fitted into the Langmuir, Freundlich, and Temkin models to study the isotherms of the process. The percentage of MB removal or removal efficiency (R%) and the amount of MB adsorbed onto the adsorbents (q_e, mg g^{-1}) were calculated using Eqs. (1) and (2), respectively. In these equations, C_0 and C_e are the starting and the equilibrium concentrations of MB in mg L^{-1}, V (L) is the volume of the examined solution, and M (g) is the mass of the utilized adsorbent.

$$R\% = \frac{\left(C_0 - C_e\right)}{C_e} \times 100 \tag{1}$$

$$q_e = \frac{V\left(C_0 - C_e\right)}{M} \tag{2}$$

The surface morphology of the prepared samples was determined by a Bruker scanning electron microscope (SEM). The crystallographic properties of the particles were unraveled through X-ray diffraction (XRD; model D8

advance) analysis. The chemical structure of the adsorbents was analyzed by making KBr pellets of the particles and recording their Fourier transform infrared (FTIR) spectra by a precise PerkinElmer spectroscope over the frequency range of 450–4,000 cm^{-1}.

For the study of the regeneration and re-adsorption of MNPs (M.C and M.AC), consecutive experiments related to the reusability and regeneration of these adsorbents were performed in several adsorption/desorption cycles. To each cycle, 0.5 g of each adsorbent was added to 50 ppm MB solution for 45 min at pH 7 to reach the adsorption equilibrium. Then, to desorb it, we used 50 mL of 0.1 M NaOH for 180 min and to neutralize and prepare the adsorbent for adsorption, we washed them with ultrapure water in several stages.

3. Results and discussion

3.1. Characterization of the adsorbents

Fig. 1 shows the SEM images of the modified AC and zeolite particles. As it can be seen, the iron oxide NPs are well stabilized on the AC and zeolite particles, so that some iron oxide particles have filled some active sites and pores of the AC and zeolite particles, which has resulted in an enhancement in their porosity and provision of smaller pores. Such changes are expected to improve the removal efficiency of the AC and zeolite adsorbents. The particle size of the obtained nano-adsorbents falls in the range of 10–90 nm.

FTIR analysis was performed on the four unmodified and modified samples to identify their functional groups and chemical compositions. Fig. 2 displays the corresponding FTIR spectra. In this figure, the broad peak observed from 3,300 to 3,500 cm^{-1} in the spectra of all samples was related to the stretching vibrations of the surficial OH groups and the adsorbed water molecules. The vibrational band positioned at 1,600 cm^{-1} in the spectra of both activated carbon and clinoptilolite refers to the stretching vibrations of the surficial C=O groups. This peak can be clearly seen in the spectra of the unmodified and modified clinoptilolite samples. However, in the case of AC, its intensity was higher for the modified sample rather than the unmodified particles.

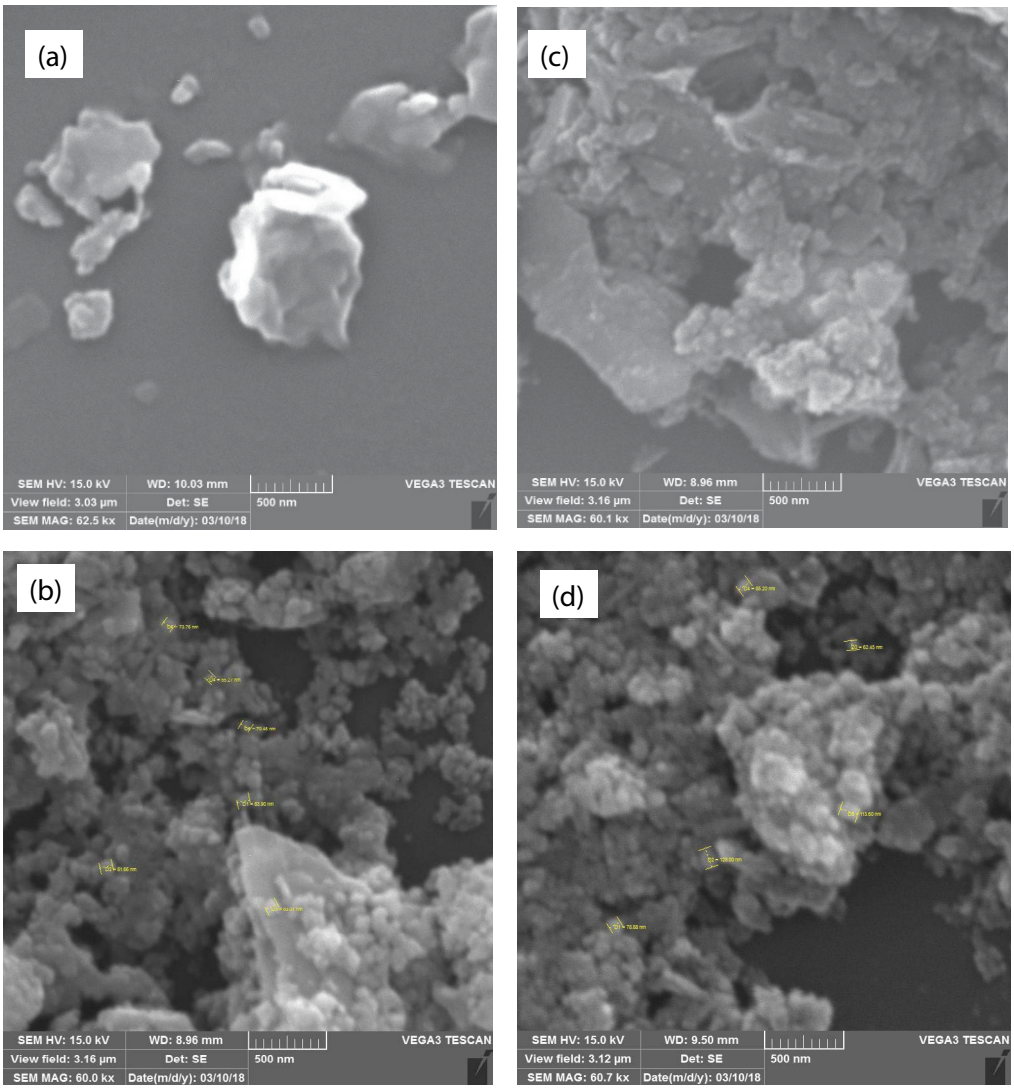

Fig. 1. SEM images of the natural (a) modified clinoptilolite, (b) unmodified, (c) activated carbon, and (d) samples.

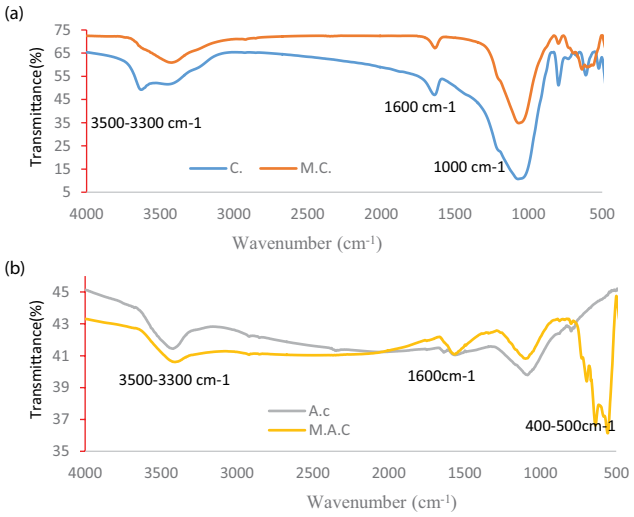

Fig. 2. FTIR spectra of the (a) unmodified and (b) modified activated carbon and clinoptilolite samples.

It is worth mentioning that the peak positioned over the range of 400–500 cm^{-1} is just detected in the modified samples and represents Fe–O bond vibrations. The presence of this peak confirms successful coating of the iron oxide NPs on the AC and zeolite particles [23].

Fig. 3 exhibits the XRD patterns of the four adsorbent samples. According to this figure, the XRD pattern of the modified zeolite particles was consistent with the standard diffraction peaks of iron oxide NPs. Furthermore, the presence of the 30.5°, 36°, 43°, 47°, and 63° peaks that correspond to cubic Fe_2O_3 crystals indicates that Fe_2O_3 MNPs have been successfully deposited on the AC and clinoptilolite particles [24]. Moreover, this figure highlights a relatively sharp peak at 22° and a peak around 27° as the characteristic peaks of the clinoptilolite and AC crystals, respectively. In general, the XRD patterns confirm deposition of the iron oxide MNPs on the studied particles.

Analysis of the specific superficial area of the synthesized magnetic nanoparticles showed that BET surface area of AC magnetic nanoparticles adsorbent was reduced as compared with non-magnetic AC. It can be due to the high porosity of the active carbon structure and presence of Fe_2O_3 nanoparticles in its porosity [12]. Previous studies have reported that the oxidation action of ferric salt played a role as an activating agent for carbon materials, as Luo et al. [25] reported that the BET surface area of the carbon composite due rice husk was detected to be 269.43 $m^2\ g^{-1}$, which was smaller than that of the non-magnetic rice husk carbon (384.18 $m^2\ g^{-1}$). The authors have concluded that the formation of Fe_3O_4 nanoparticles not only contributed to a reduction in BET surface area and pore volume but also reflected an increase in the average pore diameter [25]. Based on another BET analysis, the specific surface area of the modified zeolite by magnetic nanoparticles and the total pore volume have an increasing tendency in comparison with natural zeolite. This is due to the low porosity of clinoptilolite particles. This result is also confirmed in the study of Mockovčiaková et al. [26].

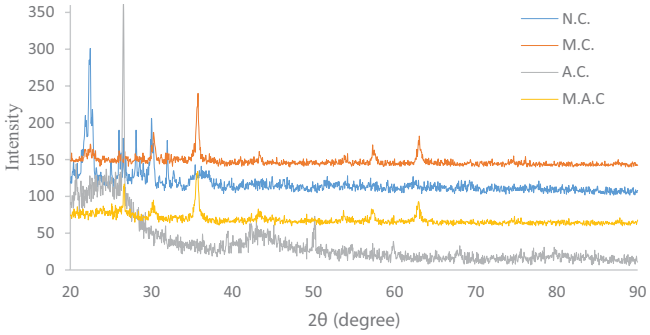

Fig. 3. XRD patterns of the activated carbon and clinoptilolite particles before and after modification by iron oxide magnetic nanoparticles.

3.2. Effect of adsorbent dose in dye removal

The effect of the adsorbent dose in the removal of 50 ppm MB by the zeolite and AC magnetic particles was evaluated at pH 7 within 45 min. For this purpose, 0.1–1 g of each adsorbent was added to 50 mL MB solution. The observed removal efficiencies are depicted in Fig. 4. As shown in this figure, increasing the amount of the modified zeolite and AC NPs from 0.1 to 1 g (2–20 g L^{-1}) increased the percentage of MB removal from 94.5% to 99.9% and from 87.2% to 99.64%, respectively. According to these values, even adsorbent doses as low as 0.2 g per 50 mL can remove a noticeable amount of the dye molecules, which indicates that these two adsorbents are highly efficient in the adsorption of organic dyes. However, adding a greater quantity of the adsorbents promotes the dye removal due to the availability of more active sites for adsorption of the MB molecules. The other point is that the modified zeolite NPs are more efficient than the modified AC particles at lower adsorbent doses. The reason might be attributed to the possession of the more active sites by the zeolite MNPs. Also, the ion exchange property of the zeolite MNPs and their surficial negative charge should have been effective on their higher removal efficiency. Another point is the trend of removal efficiency. Though increasing the dose to 0.3 g enhances the MB removal, the removal trend smoothens at 0.5 g. This observation can be explained with respect to the fact that some active sites remain unsaturated at higher adsorbent doses and their presence does not affect the removal process. Therefore, 0.5 g adsorbent in 50 mL solution was selected as the optimal dose.

3.3. Effect of pH in dye removal

In adsorption processes, pH plays a key role in increasing the adsorption capacity by varying the surface properties of the adsorbents and their ionization extent [27]. Fig. 5 illustrates the effect of pH on the adsorptive removal of 50 ppm MB by 0.5 g AC and zeolite MNPs within 45 min. Though this figure links the maximum extent of solution decolorization to acidic pH (pH = 3), the removal efficiency value does not significantly change with the increase of pH. Such behavior is in contrast with the observation of many other researchers, including Chen et al. [28], who adsorbed MB on the iron oxide coated silica and observed higher

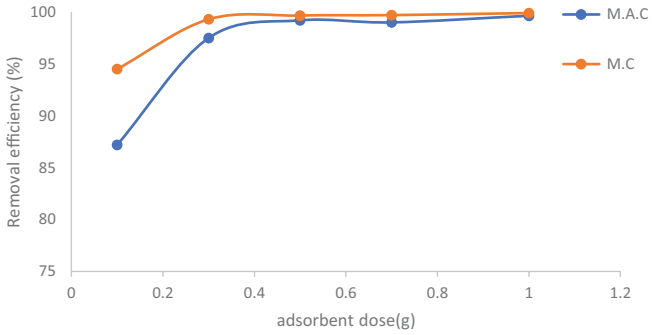

Fig. 4. Effect of adsorbent dose in MB removal by the activated carbon and clinoptilolite magnetic nanoparticles.

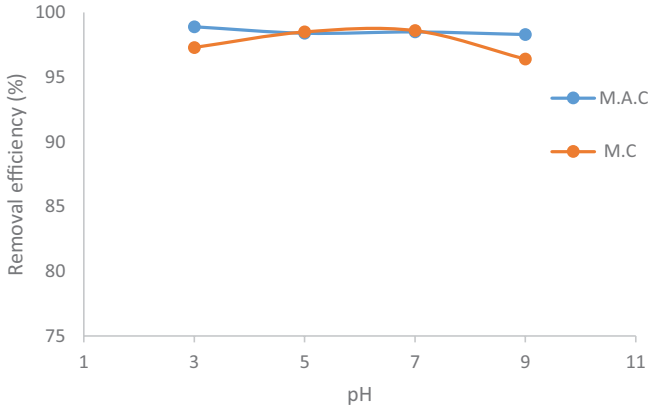

Fig. 5. Effect of pH in methylene blue removal by the activated carbon and zeolite magnetic nanoparticles.

removal efficiencies at pH levels above 6.5. Also, the study conducted by Nasrullah et al. [29] on the adsorptive removal of MB by alginate–AC grains showed that the removal of MB decreased at lower pH levels due to the existence of the H^+ ions in the solution. Therefore, insensitivity of the AC and zeolite MNPs to pH can be considered as one of the advantages of the proposed adsorbents as they can be applied to various pH conditions with negligible loss of activity.

The zero-point charge (pH_{zpc}) of the adsorbents was determined. The pH > pH_{zpc} helps increase the adsorption of cations, while the pH < pH_{zpc} helps enhance the adsorption of anions [30]. The results showed that the pH_{zpc} for the M.C and M.A.C adsorbents was 2. Therefore, the solution pH was higher than pH_{zpc}, and the absorbent surface had a negative charge; since MB is a cationic dye, adsorption in pH = 3–9 was well done. These results show that electrostatic binding between the absorbent and pollutant would increase the removal efficiency. Fig. 6 shows that MB molecules are adsorbed onto the adsorbent intermediate surfaces and pores.

To explain the pH insensitivity of AC, one should note that the pores and overall physical structure of AC, not its chemical properties, determine its adsorption capacity. In the case of the clinoptilolite MNPs, however, the situation is rather different. The efficiency of MB removal is lower at acidic pH and maximizes by increasing pH to 5 and 7. Lower

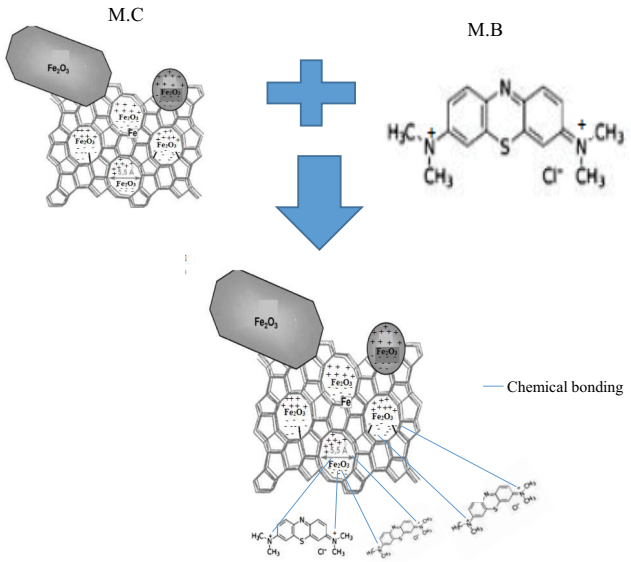

Fig. 6. Possible mechanism for adsorption of MB by Fe_2O_3@C (M.C).

adsorption of MB on the modified zeolite at acidic pH levels can be associated with the competition of protons with the cationic group of MB in accessing the adsorption sites [3]. On the other hand, at acidic pH, the OH^- ions form a complex with the other ions including the MB molecules and reduce their adsorptive removal by the zeolite MNPs [3,5]. The difference between the responses of the two adsorbents to pH roots is the fact that clinoptilolite is a cationic ion exchanger with the negative surficial charge, the combination of which with iron oxide NPs increases its adsorption capacity by producing very fine particles [22]. Since pH variations lead to chemical changes in the active sites and ionization of different functional groups, altering the pH can change the surface charge of the adsorbent particles and influence their adsorption capacity.

3.4. *Effect of the contact time of the adsorption*

Three consequent steps of mass transfer happen simultaneously with adsorption of a pollutant onto a porous adsorbent. The first step is fluid and pollutant film diffusion. In the next step, the solvent and dye molecules diffuse from the surface of the adsorbent particles toward their internal pores. In the last step, the adsorbate is adsorbed on the internal active sites. This process requires a relatively long time [3,31]. As it can be seen in Fig. 7, prolonging the contact time from 5 to 90 min. increases the removal efficiency of the unmodified zeolite and AC from 33% to 54.8% and from 32% to 61%, respectively. At 45 min, both adsorbents remove 45% of the MB molecules, while modification of the zeolite and AC particles with the iron oxide NPs, respectively, gives 98.3% and 99% MB removal at the equilibration time of 45 min. It means that coating with iron oxide improves the adsorption capacity of both adsorbents noticeably.

According to Fig. 7, the greatest extent of MB removal by the zeolite MNPs occurs within 15 min, at the beginning of the process, while the highest removal efficiency by the AC

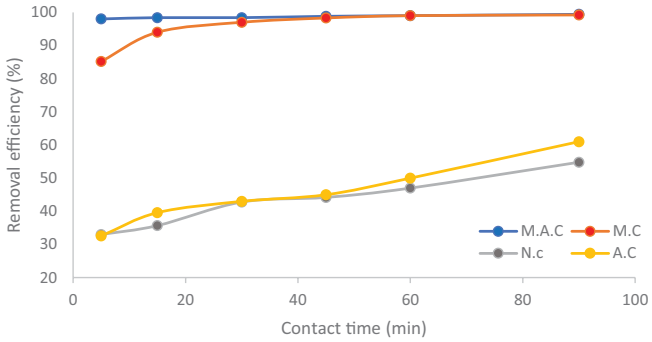

Fig. 7. Effect of contact time in the removal of 50 ppm methylene blue from a 50 mL solution containing 0.5 g activated carbon and clinoptilolite magnetic nanoparticles at pH 7.

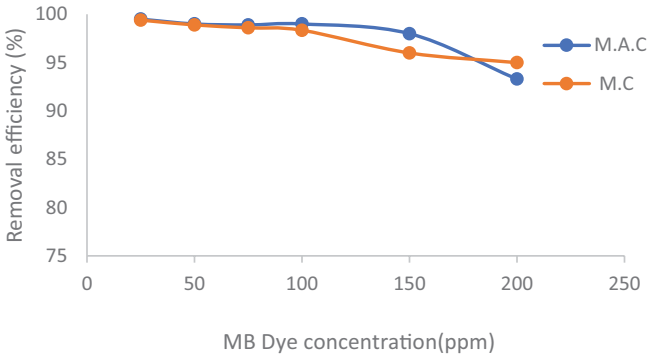

Fig. 8. Effect of initial concentration of methylene blue in adsorption efficiency of the activated carbon and clinoptilolite MNPs.

MNPs happens within the first 5 min. The reason is that there are more dye molecules with a high rate of mass transfer toward the adsorbent surface at the initial stage of the adsorption process. However, as time passes, the adsorbent sites are saturated with the MB molecules and the number of available active sites and free MB molecules reduces [32]. The superior activity of the AC MNPs suggests that its NPs are mainly composed of large pores, which enable it to adsorb the dye molecules immediately. On the other hand, the pores of the zeolite MNPs seem to be as small as or smaller than the MB molecules, which results in requiring a longer time for MB adsorption and equilibration. Even though initial adsorption of MB onto the zeolite MNPs requires a longer time compared with the AC MNPs, its equilibration time for MB adsorption (45 min) is much shorter than that of carbon–alginate carbonate (about 8 h) [3] and iron oxide modified silica (about 1.5 h) [28].

3.5. Effect of initial dye concentration on adsorption

The increase of initial dye concentration has a key role in solutions since it acts as a driving force in overcoming the resistance against mass transport between the solution and adsorbent surface. Therefore, this factor controls the equilibration of the dye molecules with the adsorbent particles [28]. Fig. 8 depicts the adsorption of various dye concentrations (25–200 ppm) on 0.5 g of the clinoptilolite and AC MNPs at pH 7 within 45 min in 50 mL of MB. It can be observed from this figure that increasing the initial concentration of MB leads to a slight decrease in the adsorption efficiency of both adsorbents. The decrease of the removal percentage from 99% to 95% is due to the accumulation of charge on the surface of the MNPs, which leads to the fast occupation of the adsorption sites and, therefore, restriction of MB diffusion toward the sites located deep inside the particles.

For the study of the regeneration of M.C and M.A.C, several adsorption–desorption cycles were made. As was previously mentioned, the MB removal rate was more than 98% with fresh M.A.C and M.C, and after first adsorption–desorption cycles, the MB removal rate was 87.5% and 83% for M.C and M.A.C, respectively. These confirm the fact that the existing chemical bonds are somewhat weak [33]. However, the contact time duration of adsorbents with NaOH was long; therefore, some adsorption sites decrease due to stronger chemical bonds.

3.6. Adsorption isotherm

Adsorption isotherms are the equations that describe the status of adsorbate equilibration between solid and liquid phases and facilitate assessment of adsorption processes [34]. In this study, the process of MB adsorption on the examined adsorbents was analyzed in the framework of the Langmuir, Freundlich, Dubinin–Radushkevich, and Temkin isotherms. The fitness of the adsorption data into the three isotherms was evaluated using the associated regression coefficients (R^2).

In general, the Langmuir isotherm supposes that the adsorbent surface is covered by homogeneous adsorption sites with equal energies and considers that the adsorbed molecules do not interact with each other. This isotherm can be written by the following relationship [29]:

$$\frac{C_e}{q_e} = \frac{1}{bQ_0} + \frac{1}{Q_0} \times C_e \tag{3}$$

where C_e (mg L^{-1}) is the equilibrium concentration of the MB molecules adsorbed onto the AC and zeolite MNPs, b (L mg^{-1}) is the constant of the Langmuir isotherm that is related to adsorption heat, Q_0 (mg g^{-1}) is the maximum adsorption capacity, and q_e (mg g^{-1}) is the amount of MB adsorbed on the adsorbents [29].

The isotherm parameters extracted by plotting the above linear equation are outlined in Table 1. As shown in the table, the q_m value of the modified clinoptilolite NPs was 52 mg g^{-1} that is greater than that of the modified AC NPs, that is, 35 mg g^{-1}. The comparison of different adsorbents for MB adsorption in Table 2 shows that M.C and M.A.C adsorbents used in this study had a further adsorption capacity compared with some adsorbents reported in other studies. The reason is that the clinoptilolite MNPs have a greater surface area and more pores, according to the SEM images. The extracted Langmuir parameters were used to calculate the R_L factor based on the following equation:

$$R_L = \frac{1}{1 + bc_0} \tag{4}$$

Table 1
Isotherm parameters of methylene blue adsorption onto the clinoptilolite and activated carbon magnetic nanoparticles

Adsorbent	Langmuir			Freundlich			Temkin			Dubinin–Radushkevich			
	q_m (mg g^{-1})	K_L (L mg^{-1})	R^2	N	K_f	R^2	A	B	R^2	X'_m (mg g^{-1})	K' mol^2 kJ^{-2})	E (kJ mol^{-1})	R^2
M.A.C	35	0.23	0.955	0.749	5.6	0.929	1.7	15.5	0	4.65	0.0011	10.6	0.836
M.C	52	0.09	0.873	0.338	2	0.972	16.6	22.7	0.823	4.66	0.0012	10.2	0.774

The R_L values can indicate the favorability of MB adsorption onto the studied adsorbents, so that R_L values greater than unity represent unfavorable adsorption, and zero R_L shows irreversibility of the process; also, the values lying in the range of zero to unity demonstrate favorable adsorption [3]. Since the obtained R_L values of the AC and zeolite MNPs were 0.23 and 0.09, respectively, the studied adsorption reactions are favorable.

The Freundlich equation is an empirical model that expresses the physisorption of the adsorbates on adsorbent materials. This model presumes multi-layer adsorption on a heterogeneous surface and concerns exponential reduction of the adsorption energy with the increase of adsorbed molecules [35,36]. The linear form of this model is as follows:

$$\log_{10} q_e = \log_{10} K_f + \frac{1}{n}\log_{10} C_e \tag{5}$$

Here, K_f is the Freundlich constant that depends on the adsorption capacity of the adsorbents and $1/n$ refers to adsorption intensity [27].

The Temkin relationship can be expressed using the following equation, in which A and B are the Temkin constants. The values of these constants are presented in Table 1.

$$q_e = A + B \ln C_e \tag{6}$$

According to the obtained R^2 values, adsorption of MB onto the AC (R^2 = 0.92) and clinoptilolite (R^2 = 0.972) MNPs is more consistent with the Freundlich model (Fig. 9). It means that the surface of the synthesized adsorbents is inhomogeneous and a portion of the process involves local adsorption rather than layered MB adsorption. A similar study on arsenic adsorption onto the 0.5 g L^{-1} adsorbent has also reported the consistency of the observed process with the Freundlich isotherm [22].

Dubinin–Radushkevich isotherm is an empirical model that is applied to express the adsorption mechanism [37]. Isotherm is generally expressed as follows:

$$\ln q_e = \ln X'_m - K' \varepsilon^2 \tag{7}$$

where ε = Polanyi potential (ε = RT ln (1 + (1/C_e))); R = universal gas constant (J deg^{-1} mol^{-1}); T = temperature in Kelvin; C_e = equilibrium concentration (ppm); q_e = equilibrium amount adsorbed (mg g^{-1}); X'_m = adsorption capacity (mg g^{-1}); K' = constant related to the energy of adsorption (mol^2 kJ^{-2}). This approach was used to determine the physical and chemical adsorption processes of MB with its mean free energy; E per molecule of the adsorbate can be computed using the following equation [37,38]:

$$E = \frac{1}{\sqrt{-2K'}} \tag{8}$$

The adsorption apparent energy and Dubinin–Radushkevich isotherm constants are shown in Table 1. If the E magnitude between 8 and 16 (kJ mol^{-1}) shows that the adsorption follows a chemical process, while the values of E less than 8 (kJ mol^{-1}), the adsorption process is a physical nature [39-42]. On the basis of the Dubinin–Radushkevich isotherm, this internal adsorption is a chemical bond.

Table 2
Comparison of M.C and M.A.C adsorption capacity with other adsorptions in some previous studies for MB adsorption

Adsorbent	Adsorption capacity (mg g^{-1})	Optimal pH	Adsorbent dose (g L^{-1})	Equilibration time	References
Banana peel	20.8 mg g^{-1}	7.2	1	24 h	[37]
Modified zeolite	8.7	6.43	0.1	30 min	[39]
Carbon–alginate composite	35.9	8	10	8 h	[40]
Magnetic γFe_2O_3/SiO_2 nanocomposite	18.4	7	1	30 min	[28]
Zeolite	1.3	5	1	10 min	[43]
Beer brewery waste	4.92	7	0.25	24 h	[44]
Activated carbon of *Nasturtium microphyllum*	67.5	7	0.8	0.5 h	[45]
Natural zeolite	23.6	6.7	0.01–0.05	1,000 min	[46]
M.C	52	7	10	45 min	Present study
M.A.C	35	7	10	45 min	Present study

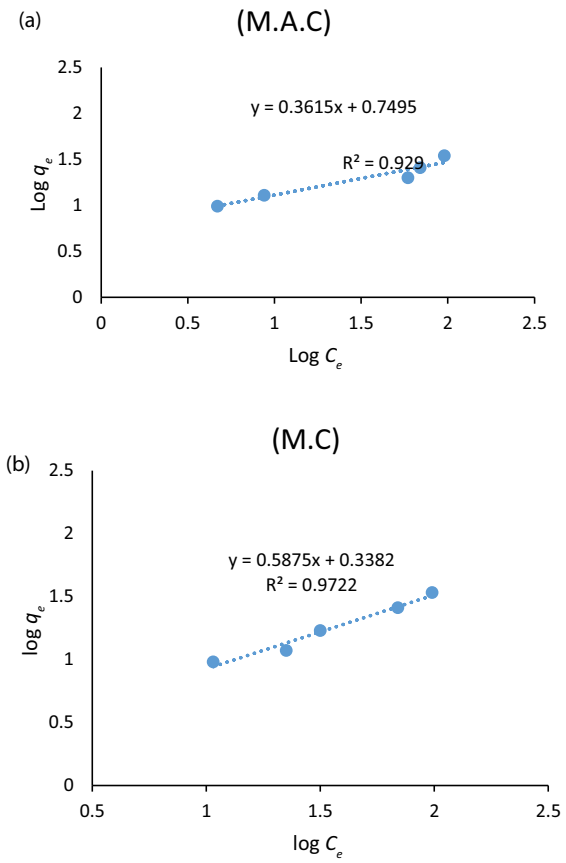

Fig. 9. Isotherms of methylene blue adsorption onto the (a) activated carbon and (b) clinoptilolite magnetic nanoparticles.

4. Conclusion

According to the physiochemical properties of the modified activate carbon and zeolite particles, the Fe_2O_3 nanoparticles have completely covered the surface of the adsorbent structures and have led to an increase in their porosity. The results showed that the adsorption process was affected by contact time, adsorbent dose, and initial methylene blue concentration. The activated carbon magnetic nanoparticles equilibrated in a shorter time compared with the clinoptilolite magnetic nanoparticles. Based on the results of this study, the application of 0.5 g modified activated carbon and clinoptilolite nanoparticles to the removal of 100 ppm methylene blue results in 99% and 98.35% removal efficiency, respectively. The corresponding adsorption processes are more consistent with the Freundlich isotherm. Furthermore, the capacity of the activated carbon and clinoptilolite magnetic nanoparticles for adsorption of methylene blue is 35 and 52 mg g^{-1}, respectively. Therefore, it can be concluded that both adsorbents are highly efficient in removing the methylene blue from the dye containing wastewaters.

Acknowledgments

The authors would like to thank the Deputy of Research of Shiraz University of Medical Sciences for their financial support. The authors wish to thank Dr. Shokrpour at the Research Consultation Center (RCC) of Shiraz University of Medical Sciences for her invaluable assistance in editing this manuscript.

References

[1] M.R. Samarghandi, M. Zarrabi, A. Amrane, G.H. Safari, S. Bashiri, Application of acidic treated pumice as an adsorbent for the removal of azo dye from aqueous solutions: kinetic, equilibrium and thermodynamic studies, Iran. J. Environ. Health Sci. Eng., 9 (2012) 1–9.
[2] A.K. Kushwaha, N. Gupta, M.C. Chattopadhyaya, Removal of cationic methylene blue and malachite green dyes from aqueous solution by waste materials of *Daucus carota*, J. Saudi Chem. Soc., 18 (2014) 200–207.
[3] A.F. Hassan, A.M. Abdel-Mohsen, M.M.G. Fouda, Comparative study of calcium alginate, activated carbon, and their composite beads on methylene blue adsorption, Carbohydr. Polym., 102 (2014) 192–198.
[4] J.-Z. Yi, L.-M. Zhang, Removal of methylene blue dye from aqueous solution by adsorption onto sodium humate/polyacrylamide/clay hybrid hydrogels, Bioresour. Technol., 99 (2008) 2182–2186.
[5] F.A. Pavan, A.C. Mazzocato, Y. Gushikem, Removal of methylene blue dye from aqueous solutions by adsorption using yellow passion fruit peel as adsorbent, Bioresour. Technol., 99 (2008) 3162–3165.
[6] L. Wang, J. Zhang, A. Wang, Removal of methylene blue from aqueous solution using chitosan-*g*-poly(acrylic acid)/montmorillonite superadsorbent nanocomposite, Colloids Surf., A, 322 (2008) 47–53.
[7] L. Wang, J. Zhang, A. Wang, Fast removal of methylene blue from aqueous solution by adsorption onto chitosan-*g*-poly(acrylic acid)/attapulgite composite, Desalination, 266 (2011) 33–39.
[8] M. Changmai, M.K. Purkait, Kinetics, equilibrium and thermodynamic study of phenol adsorption using $NiFe_2O_4$ nanoparticles aggregated on PAC, J. Water Process Eng., 16 (2017) 90–97.
[9] G. Gangadhar, U. Maheshwari, S. Gupta, Application of nanomaterials for the removal of pollutants from effluent streams, J. Nanosci. Nanotechnol., 2 (2012) 140–150.
[10] M. Changmai, P. Banerjee, K. Nahar, M.K. Purkait, A novel adsorbent from carrot, tomato and polyethylene terephthalate waste as a potential adsorbent for Co (II) from aqueous solution: kinetic and equilibrium studies, J. Environ. Chem. Eng., 6 (2018) 246–257.
[11] S. Dehestaniathar, A. Rezaee, Adsorption of nitrate from aqueous solution using activated carbon-supported Fe^0, $Fe_2(SO_4)_3$, and $FeSO_4$, J. Adv. Environ. Health Res., 2 (2014) 36–43.
[12] B. Kakavandi, A.J. Jonidi, R.K. Rezaei, S. Nasseri, A. Ameri, A. Esrafily, Synthesis and properties of Fe_3O_4-activated carbon magnetic nanoparticles for removal of aniline from aqueous solution: equilibrium, kinetic and thermodynamic studies, Iran. J. Environ. Health Sci. Eng., 10 (2013) 1–9.
[13] M.H. Do, N.H. Phan, T.D. Nguyen, T.T.S. Pham, V.K. Nguyen, T.T. Vu, T.K.P. Nguyen, Activated carbon/Fe_3O_4 nanoparticle composite: Fabrication, methyl orange removal and regeneration by hydrogen peroxide, Chemosphere, 85 (2011) 1269–1276.
[14] E. Shahnazari-Shahrezaie, A. Nezamzadeh-Ejhieh, A zeolite modified carbon paste electrode based on copper exchanged clinoptilolite nanoparticles for voltammetric determination of metronidazole, RSC Adv., 23 (2017) 14247–14253.
[15] Z. Deng, M. Liang, H. Li, Z. Zhu, Advances in Preparation of Modified Activated Carbon and its Applications in the Removal of Chromium (VI) from Aqueous Solutions, IOP Conference Series: Earth and Environmental Science, IOP Publishing, Shanghai, China, 2016, pp. 132–141.
[16] M. Ghaedi, H. Karimi, F. Yousefi, Silver and zinc oxide nanostructures loaded on activated carbon as new adsorbents for removal of methylene green: a comparative study, Hum. Exp. Toxicol., 33 (2014) 956–967.

[17] P.L. Hariani, M. Faizal, Ridwan, Marsi, D. Setiabudidaya, Removal of Procion Red MX-5B from songket's industrial wastewater in South Sumatra Indonesia using activated carbon-Fe_3O_4 composite, Sustainable Environ. Res., 28 (2018) 158–164.
[18] J. Liu, Y. Wang, Y. Fang, T. Mwamulima, S. Song, C. Peng, Removal of crystal violet and methylene blue from aqueous solutions using the fly ash-based adsorbent material-supported zero-valent iron, J. Mol. Liq., 250 (2018) 468–467.
[19] W.C. Qian, X.P. Luo, X. Wang, M. Guo, B. Li, Removal of methylene blue from aqueous solution by modified bamboo hydrochar, Ecotoxicol. Environ. Saf., 157 (2018) 300–306.
[20] A.R. Satayeva, C.A. Howell, A.V. Korobeinyk, J. Jandosov, V.J. Inglezakis, Z.A. Mansurov, S.V. Mikhalovsky, Investigation of rice husk derived activated carbon for removal of nitrate contamination from water, Sci. Total Environ., 630 (2018) 1237–1245.
[21] U. Pal, A. Sandoval, S.I.U. Madrid, G. Corro, V. Sharma, P. Mohanty, Mixed titanium, silicon, and aluminum oxide nanostructures as novel adsorbent for removal of rhodamine 6G and methylene blue as cationic dyes from aqueous solution, Chemosphere, 163 (2016) 142–152.
[22] A.T.M. Salem, X.L. Hu, D.Q. Yin, Synthesised magnetic nanoparticles coated zeolite (MNCZ) for the removal of arsenic (As) from aqueous solution, J. Exp. Nanosci., 9 (2014) 551–560.
[23] J. Saini, V.K. Garg, R.K. Gupta, Removal of Methylene Blue from aqueous solution by Fe_3O_4@Ag/SiO_2 nanospheres: synthesis, characterization and adsorption performance, J. Mol. Liq., 250 (2018) 413–422.
[24] Z. Mahmoudi, S. Azizian, B. Lorestani, Removal of methylene blue from aqueous solution: a comparison between adsorption by iron oxide nanospheres and ultrasonic degradation, J. Mater. Environ., 5 (2014) 1332–1335.
[25] S. Luo, M.-N. Shen, F. Wang, Q.-R. Zeng, J.-H. Shao, J.-D. Gu, Synthesis of Fe_3O_4-loaded porous carbons developed from rice husk for removal of arsenate from aqueous solution, Int. J. Environ. Sci. Technol., 13 (2016) 1137–1148.
[26] A. Mockovčiaková, Z. Orolínová, M. Matik, P. Hudec, E. Kmecová, Iron oxide contribution to the modification of natural zeolite, Acta Montan Slovaca, 11 (2006) 353–357.
[27] A. Seidmohammadi, G. Asgari, M. Leili, A. Dargahi, A. Mobarakian, Effectiveness of quercus branti activated carbon in removal of methylene blue from aqueous solutions, Arch. Hyg. Sci., 4 (2015) 217–225.
[28] D. Chen, Z. Zeng, Y. Zeng, F. Zhang, M. Wang, Removal of methylene blue and mechanism on magnetic γ-Fe_2O_3/SiO_2 nanocomposite from aqueous solution, Water Res. Ind., 15 (2016) 1–13.
[29] A. Nasrullah, A.H. Bhat, A. Naeem, M.H. Isa, M. Danish, High surface area mesoporous activated carbon-alginate beads for efficient removal of methylene blue, Int. J. Biol. Macromol., 107 (2018) 1792–1799.
[30] M. Zarei, N. Djafarzadeh, L. Khadir, Removal of direct blue 129 from aqueous medium using surfactant-modified zeolite: a neural network modeling, Environ. Health Eng. Manage., 5 (2018) 101–113.
[31] B. Hameed, A.T.M. Din, A.L. Ahmad, Adsorption of methylene blue onto bamboo-based activated carbon: kinetics and equilibrium studies, J. Hazard. Mater., 141 (2007) 819–825.
[32] A. Shokrolahzadeh, R.A. Shokuhi, J. Adinehvand, Modification of nano Clinoptilolite Zeolite using sulfuric Acid and its application toward removal of Arsenic from water sample, J. Nanoanalysis, 4 (2017) 48–58.
[33] S. Arivolix, M. Hema, S. Parthasarathy, N. Manju, Adsorption dynamics of methylene blue by acid activated carbon, J. Chem. Pharm. Res., 2 (2010) 626–641.
[34] M.A.M. Salleh, D.K. Mahmoud, W.A.W.A. Karim, A. Idris, Cationic and anionic dye adsorption by agricultural solid wastes: a comprehensive review, Desalination, 280 (2011) 1–13.
[35] A. Azhdarpoor, R. Nikmanesh, F. Khademi, A study of Reactive Red 198 adsorption on iron filings from aqueous solutions, Environ. Technol., 35 (2014) 2956–2960.
[36] S. Akyil, M.A.A. Aslani, M. Eral, Sorption characteristics of uranium onto composite ion exchangers, J. Radioanal. Nucl. Chem., 256 (2003) 45–51.
[37] G. Annadurai, R.S. Juang, D.J. Lee, Use of cellulose-based wastes for adsorption of dyes from aqueous solutions, J. Hazard Mater, 92 (2002) 263–74.
[38] K.Y. Foo, B.H. Hameed, Insights into the modeling of adsorption isotherm systems, Chem. Eng. J., 156 (2010) 2–10.
[39] X. Jin, M.-q. Jiang, X.-q. Shan, Z.-g. Pei, Z. Chen, Adsorption of methylene blue and orange II onto unmodified and surfactant-modified zeolite, J. Colloid Interface Sci., 328 (2008) 243–247.
[40] M.V. Dinu, M.M. Lazar, E.S. Dragan, Dual ionic cross-linked alginate/clinoptilolite composite microbeads with improved stability and enhanced sorption properties for methylene blue, React. Funct. Polym., 116 (2017) 31–40.
[41] J.A. Lori, A.O. Lawal, E.J. Ekanem, Adsorption characteristics of active carbons from pyrolysis of bagasse, sorghum and millet straws in ortho phosphoric acid, Environ. Sci. Technol., 1 (2008) 124–134.
[42] I.O. Brahim, M. Belmedani, A. Belgacem, H. Hadoun, Z. Sadaoui, Discoloration of azo dye solutions by adsorption on activated carbon prepared from the cryogenic grinding of used tires, Chem. Eng. Trans., 38 (2014) 121–126.
[43] D.A. Fungaro, L.C. Grosche, A. Pinheiro, J. de Carvalho Izidoro, S. Borrely, Adsorption of methylene blue from aqueous solution on zeolitic material for color and toxicity removal, Orbital: Electron. J. Chem., 2 (2011) 235–247.
[44] W.T. Tsai, H.C. Hsu, T.Y. Su, K.Y. Lin, C.M. Lin, Removal of basic dye (methylene blue) from wastewaters utilizing beer brewery waste, J. Hazard. Mater., 154 (2008) 73–78.
[45] S. Mousavi, M. Mehralian, M. Khashij, S. Parvaneh, Methylene Blue removal from aqueous solutions by activated carbon prepared from N. microphyllum (AC-NM): RSM analysis, isotherms and kinetic studies, Global Nest J., 19 (2017) 697–705.
[46] F. Jafari-zare, A. Habibi-yangjeh, Competitive adsorption of methylene blue and rhodamine B on natural zeolite: thermodynamic and kinetic studies, Chinese J. Chem., 28 (2010) 346–359.